Geophysical Research Letters

RESEARCH LETTER
10.1029/2022GL102468

Key Points:

- Unique coincident and collocated airborne observations of Sea Surface Temperature, surface currents and properties of surface waves across submesoscales features
- A new airborne instrument enables observations of surface currents, vertical and horizontal shear to capture quickly evolving ocean features
- Such observations are crucial to develop better understanding of the physics of submesoscale processes and wave-current interaction

Correspondence to:
L. Lenain,
llenain@ucsd.edu

Citation:
Lenain, L., Smeltzer, B. K., Pizzo, N., Freilich, M., Colosi, L., Ellingsen, S. Å., et al. (2023). Airborne remote sensing of upper-ocean and surface properties, currents and their gradients from meso to submesoscales. *Geophysical Research Letters*, *50*, e2022GL102468. https://doi.org/10.1029/2022GL102468

Received 22 DEC 2022
Accepted 6 APR 2023

Airborne Remote Sensing of Upper-Ocean and Surface Properties, Currents and Their Gradients From Meso to Submesoscales

Luc Lenain[1], Benjamin K. Smeltzer[2,3], Nick Pizzo[1], Mara Freilich[1,4], Luke Colosi[1], Simen Å. Ellingsen[2], Laurent Grare[1], Hugo Peyriere[1], and Nick Statom[1]

[1]Scripps Institution of Oceanography, University of California San Diego, La Jolla, CA, USA, [2]Department of Energy Process Engineering, Norwegian University of Science and Technology, Trondheim, Norway, [3]Marinteknisk senter, SINTEF Ocean, Trondheim, Norway, [4]Department of Earth, Environmental and Planetary Science, Division of Applied Mathematics, Brown University, Providence, RI, USA

Abstract In this work we present a unique set of coincident and collocated high-resolution observations of surface currents and directional properties of surface waves collected from an airborne instrument, the Modular Aerial Sensing System, collected off the coast of Southern California. High-resolution observations of near surface current profiles and shear are obtained using a new instrument, "DoppVis", capable of capturing horizontal spatial current variability down to 128 m resolution. This data set provides a unique opportunity to examine how currents at scales ranging from 1 to 100 km modulate bulk (e.g., significant wave height), directional and spectral properties of surface gravity waves. Such observations are a step toward developing better understanding of the underlying physics of submesoscale processes (e.g., frontogenesis and frontal arrest) and the nature of transitions between mesoscale and submesoscale dynamics.

Plain Language Summary In recent years, through improvement of computational resolution of global ocean models, scientists have begun to suspect that kilometer-scale eddies, whirlpools and fronts, called "submesoscale" variability, make important contributions to horizontal and vertical exchange of climate and biological variables in the upper ocean. Such features are challenging to analyze, because of their size (and how quickly they evolve; within hours), they are too large to study from a research vessel but smaller than regions typically studied with satellite measurements. In this work, we use a research aircraft instrumented to characterize ocean currents, temperature, color (in turn chlorophyll concentration) and the properties of surface waves over an area large enough to capture submesoscale processes. This approach is a step forward in understanding and quantifying the underlying physics of submesoscale processes, and in turn develops parameterization that can help improve the fidelity of weather and climate models.

1. Introduction

The transfer of mass, momentum, and energy between the atmosphere and ocean are complex due to their interactions across a broad range of space and time scales (Melville, 1996). A better understanding of the physics of these processes is fundamental for improved parameterizations used in coupled air-sea models of weather and climate, particularly as Earth's climate changes (Cavaleri et al., 2012). For example, although the importance of surface waves in these models has long been acknowledged, only relatively recently have global models included physics-based models of their effects (see, e.g., Li et al., 2016; Sullivan & McWilliams, 2010). Specifically, the effects of the non-breaking surface wave induced transport that catalyzes Langmuir circulations have been shown to reduce errors in sea surface temperature (Belcher et al., 2012), crucial to climate modeling.

At slightly larger scales, but still well smaller than the resolution of climate models, submesoscale ocean currents have horizontal scales on the order of 0.1–10 km and have recently been hypothesized to make important contributions to vertical exchanges of climate and biological variables in the upper ocean (Mahadevan, 2016) as well as provide a pathway from energetically rich large scale flows to small scale dissipation (Balwada et al., 2022; Srinivasan et al., 2023). Model studies and limited observations (e.g., D'Asaro et al., 2018) show that submesoscale vertical exchange is concentrated near kilometer-scale fronts, jets, and eddies (McWilliams, 2016). Submesoscale physics are at the smallest scales that have been resolved in global ocean models, where their net effect on heat exchange between the ocean and atmosphere has shown to be much larger than mesoscale eddies (Su

et al., 2018). However, these simulations are sensitive to the parameterized physics of the smaller scale motion, including waves, which remains poorly understood. To address the fundamental questions of the observed nature of submesoscale dynamics and the interactions between submesoscale dynamics and smaller scale surface wave processes, a comprehensive set of novel, coincident and collocated measurements of the dynamical variables is needed to improve state-of-the-art high-resolution simulations of weather and climate, and better understand vertical exchanges of heat and biogeochemical tracers.

Due to non-linear coupling between oceanic and atmospheric processes, including currents, winds, and waves, coincident observations are necessary to understand these dynamics. A number of model and observational studies have demonstrated the variety of ways by which air-sea interaction can induce horizontal divergence of surface currents and thus force vertical velocities. Coincident observations of surface vector winds and currents are needed to better understand the coupling of winds and currents and in turn improve surface flux parameterizations (Bourassa et al., 2019). The wind stress can be modified by Sea Surface Temperature (SST) and velocity gradients (Chelton et al., 2004; Dewar & Flierl, 1987; Fairall et al., 1996; O'Neill et al., 2005) while the resulting convergence of the ocean Ekman layer can be modified by surface vorticity (McGillicuddy et al., 2007; Stern, 1965). At submesoscales, these effects are expected to increase in intensity. Frontal structures are strongly affected by the relative direction of the wind with *downfront* Ekman transport sharpening the fronts and inducing vertical exchange while *upfront* transport subdues the front and stratifies the upper ocean (Thomas et al., 2005). Surface waves and wave breaking can be strongly modulated at fronts (Romero et al., 2017; Vrećica et al., 2022), suggesting that even the basic formulation of air-sea exchange in terms of simple bulk coefficients will likely break down at sufficiently small scales. As such, an understanding of submesoscale structure and vertical velocity requires that air-sea interaction parameters be observed simultaneously with submesoscale measurements.

Of particular interest are observations of surface and near surface currents, wave breaking (Vrećica et al., 2022), and the directional properties of ocean surface waves. While much progress have been made on characterizing the latter (e.g., Herbers et al., 2012; Lenain & Melville, 2014, 2017; Lenain & Pizzo, 2020; Melville et al., 2016), collecting observations of near surface currents, that is, from the surface down to several meters depth, remains challenging and spatially limited in large part due to the presence of waves, which induce platform motions and additional sources of background noise. Aircraft-based observations offer a well-suited alternative due to their fast speed relative to ships and higher resolution measurements than most satellites. Previous suborbital approaches have mostly focused on radar or Synthetic Aperture Radar technologies (e.g., Nouguier et al., 2018; Rodríguez et al., 2018a, 2018b; Toporkov et al., 2005). Obtaining currents from scatterometers is not trivial, as these instruments estimate currents from measurements of short surface gravity waves that are for example, subject to modulation from longer waves (Longuet-Higgins and Stewart, 1962), a fact that is currently ignored in the way the data are processed, that generally relies on the use of an empirical geophysical model functions. Here, we circumvent these challenges by inferring current profiles remotely based on observations of the spatio-temporal evolution of surface waves that follow a dispersion relationship, a much simpler and robust approach, for the first time implemented for mapping surface current gradients at the submesoscale.

We present unique coincident and collocated high-resolution observations of the ocean surface properties collected from an airborne instrument, the Modular Aerial Sensing System (MASS), off the coast of Southern California. Central to this work is the development of a new sensor, "DoppVis," capable of measuring surface currents, their gradients and near surface vertical shear along the track of an aircraft. Velocity gradients are of particular importance for understanding submesoscale dynamics and their interactions with wind, waves, and biological processes. Computing velocity gradients from traditional velocity measurements including from ships and drifters (Essink et al., 2022; Shcherbina et al., 2013) is limited because these measurements alias quickly evolving submesoscale processes and suffer from sampling bias.

We present airborne observations that for the first time provide a snapshot of the spatial structure of ocean currents and their velocity gradient statistics from sub-kilometer to mesoscales, such as the transition between balanced and unbalanced motion, and the flow structure in vorticity-strain space. Such measurements are crucial to develop a better understanding of the underlying physics of submesoscale dynamics, and validate recent advancements made on this topic through numerical studies (Balwada et al., 2021; Callies et al., 2020).

Combined with the additional collocated and coincident observations captured by MASS (surface waves, SST, ocean color and breaking statistics in particular), we also examine how currents at scales ranging from 1 to 100 km modulate surface gravity waves, that is, bulk, directional and spectral properties.

2. Experiments

In this study we consider observations collected during two distinct experiments. The first was conducted as part of the "Platform Centric ASW Processing with Through-the-Sensor Data Assimilation and Fusion" project, funded through the ONR Task Force Ocean (TFO) initiative with the aim of collecting a simultaneous combination of acoustic, air-sea interaction and oceanographic measurements. Observations from a research vessel, a drifting instrument array, autonomous surface vehicles and a research aircraft were collected in May 2021, approximately 45 km offshore of San Diego, CA, in the vicinity of CalCoFi Line #90. One of the TFO research flights, considered in the analysis presented here, were dedicated to collecting observations across two small counter-rotating eddies separated by approximately 100 km.

The second experiment was conducted as part of the NASA S-MODE program, a project that aims to characterize the contribution of submesoscale ocean dynamics to vertical and horizontal transport in the upper ocean by employing a combination of aircraft-based remote sensing measurements of the ocean surface, in-situ measurements from research vessels and a variety of autonomous oceanographic platforms, and numerical modeling (Farrar et al., 2020). The "pilot" experiment considered here was conducted in the fall of 2021 off the coast of San Francisco, CA.

Data collected from instrumented Wave Gliders (Grare et al., 2021) and an airborne instrument, the Sea Interaction Laboratory (SIO) MASS (Melville et al., 2016) during these two field programs are considered in the analysis. During both experiments the MASS instrument was installed on a Twin Otter DHC-6 aircraft (Twin Otter International, Grand Junction, CO).

3. SIO-MASS DoppVis Instrument: Enabling Novel Airborne Observations of Near-Surface Currents

The MASS is an airborne instrument developed at the Air-SIO to simultaneously collect observations of SST and ocean color (Lenain & Pizzo, 2021; Melville et al., 2016), winds and mean-square slope (Lenain et al., 2019), surface waves (Lenain & Melville, 2017; Lenain & Pizzo, 2020), and ocean topography (Villas Bôas et al., 2022), at horizontal scales ranging from sub-meter to mesoscales. Over the past 11 years, the instrument was flown for more than 30 missions, covering a broad range of environmental conditions, locations, and applications. Details on the system performance and various applications of the MASS can be found in Lenain and Melville (2017), Lenain and Pizzo (2020), Lenain et al. (2019), Melville et al. (2016), and Vrećica et al. (2022).

In 2020, we started the development and integration of a new sensor into the MASS instrument, called "DoppVis," to obtain coincident observations of surface currents alongside the MASS observations listed above. The approach used is to infer currents from optical observations of the spatio-temporal evolution of surface waves, whose dispersion is altered by the presence of an underlying current. This technique has been primarily used with radar technology (e.g., Campana et al., 2016; Lund et al., 2015; Stewart & Joy, 1974) then later applied to airborne video imagery (Anderson et al., 2013; Dugan et al., 2001; Dugan & Piotrowski, 2003; Streßer et al., 2017).

Starting from the dispersion relation for small-amplitude linear waves propagating on top of a depth-varying current,

$$\omega(\mathbf{k}) = \omega_0(k) + \mathbf{c}(k) \cdot \mathbf{k}, \tag{1}$$

where ω is the wave frequency, ω_0 is the frequency in the absence of currents, that is, equal to $\sqrt{gk}$ in deep water, $\mathbf{k} = (k_x, k_y)$ is the wavenumber, $k = |\mathbf{k}|$, and $\mathbf{c}$ is the Doppler shift velocity due to the underlying current. Following Stewart and Joy (1974), assuming the waves are in deep-water, $\mathbf{c}$ can be approximated as a weighted average of the current profile as a function of depth such that

$$\mathbf{c}(k) = 2k \int_{-\infty}^{0} \mathbf{U}(z) e^{2kz} \mathrm{d}z, \tag{2}$$

where $\mathbf{U}(z) = (U, V)$ is the *Lagrangian* mean current profile (i.e., the current measured in an earth-fixed reference frame plus the wave-induced Stokes drift) as a function of depth z (Pizzo et al., 2022). Equation 2 is accurate to a few percent for most oceanic flows, whose vertical shear is weak to moderate (Ellingsen & Li, 2017). Based on this relationship, one can assign an effective depth z_e to the measured Doppler velocities $\mathbf{c}(k)$ by finding the

depth at which the Doppler velocity is equal to the current (Smeltzer et al., 2019; Stewart & Joy, 1974), such that $z_e(k) = -1/2k$. This is referred to as the Effective Depth Method in Smeltzer et al. (2019).

The DoppVis instrument collects visible imagery of the ocean surface using a Nikon D850 camera with 14 mm lens mounted with a 90° rotation (long edge of image parallel with flight track) and a 30° positive pitch angle from nadir (pointing slightly ahead of aircraft). The camera is synchronized to a coupled Global Positioning System/Inertial Motion Unit (GPS/IMU) system collecting images at a 2 Hz frame rate. Raw images are carefully calibrated for lens distortion and boresight misalignment with the GPS/IMU over a hard terrestrial target, then georeferenced and exported with reference to WGS84 datum with a Universal Transverse Mercator (UTM) zone 10 projection (EPSG 32610) at 50 cm horizontal resolution. Each image is then interpolated on a regular grid, to enable the generation of 3D cubes of imagery (time, UTM X, UTM Y) of set duration and dimension (N_x, N_y), where $N_x = N_y$, typically in the range of 128–512 m. The number of collected data cubes in the cross and along track direction of the aircraft varies as a function of aircraft altitude. All data presented here except for Figure 4 were collected at 1,500 ft above Mean Sea Level (AMSL), corresponding to approximately two 256×256 m^2 regions in the cross-track direction. Cube durations were typically 20–40 s. Following the same approach described in Smeltzer and Ellingsen (2021) and Smeltzer et al. (2019), all cubes of space–time data are converted to wavenumber–frequency space using a 3D Fast Fourier Transform. Doppler shift velocities are extracted from the spectrum as a function of wavenumber by masking the spectrum into wavenumber magnitude bins (bin half-width of $4\pi/N_x$), where for each bin the current $\mathbf{c}(k)$ is estimated using a normalized scalar product method (Huang et al., 2016; Streßer et al., 2017) with a Gaussian characteristic function (Smeltzer et al., 2019) peaked along the linear dispersion relation.

Figure 1a shows an example of current profiles (U, V) collected from DoppVis during an overflight of an instrumented Wave Glider during the S-MODE experiment on 4 November 2021 at 17:20 UTC. The Wave Glider was instrumented with an upward-looking Nortek Signature 1000 Acoustic Doppler Current Profiler ([ADCP], orange squares) and a downward-looking ADCP (Teledyne RDI Workhorse 300 kHz), carefully motion compensated using an onboard GPS/IMU system (Grare et al., 2021). Observations from DoppVis and the wave glider were collected within 5 min and no further than 500 m from each other to minimize any error associated with natural spatial and temporal variability. The 3D spectra were averaged in the cross-track and along-track direction (1 km bin) to improve signal-to-noise ratio. We find good agreement between in-situ and remotely sensed observations of near-surface current (U, V), with a bias = −0.014 m/s and rms deviation = 0.052 m/s, and a coefficient of determination $R^2 = 0.96$.

Finally, airborne observations of SST collected from MASS on 4 November 2021, over the entire domain along with current estimates (1 km along-track resolution) from DoppVis at two depths, $z = -1.5 \pm 0.5$ m (black arrows) and $z = -0.4 \pm 0.1$ m (red arrows) are shown in Figure 1c. Note the correlation between features present in the SST fields and the surface currents from DoppVis. Throughout the domain, we consistently find larger magnitudes of the eastern component of the current closer to the surface, likely caused by Stokes drift included in the Lagrangian current observed by DoppVis (Barrick & Weber, 1977; Broche et al., 1983; Pizzo et al., 2022). Wind and waves were coming from the west at the time of the flight.

4. Wave-Current Interactions From Meso- to Submesoscales

The collocated observations from the multiple instruments on the MASS allow for investigation of interactions between currents and other oceanographic properties such as waves, heat, and biological communities. We now examine observations collected during the "Platform Centric ASW Processing with Through-the-Sensor Data Assimilation and Fusion" TFO project in May 2021 to illustrate the importance of high spatial resolution, collocated observations for studying wave-current observations.

Several research flights were dedicated to collecting observations across two counter-rotating eddies separated by approximately 100 km. Figure 2a shows depth-averaged (0.3–2 m) surface currents (250 m along-track resolution) along with significant wave height measurements collected coincidentally with the MASS instrument. The black contours represent the sea surface height (ssh, AVISO) at the time of the observations, while corresponding surface currents from HYCOM (GOF 3.1, GLBy0.08-expt93.0) are shown as gray quivers. We find the HYCOM estimated currents to be in good agreement with DoppVis observations at the mesoscale, but strikingly miss many of the submesoscale features throughout the domain. We also find significant modulation of the surface wave properties across the domain that is not caused by temporal (e.g., inertial) variability.

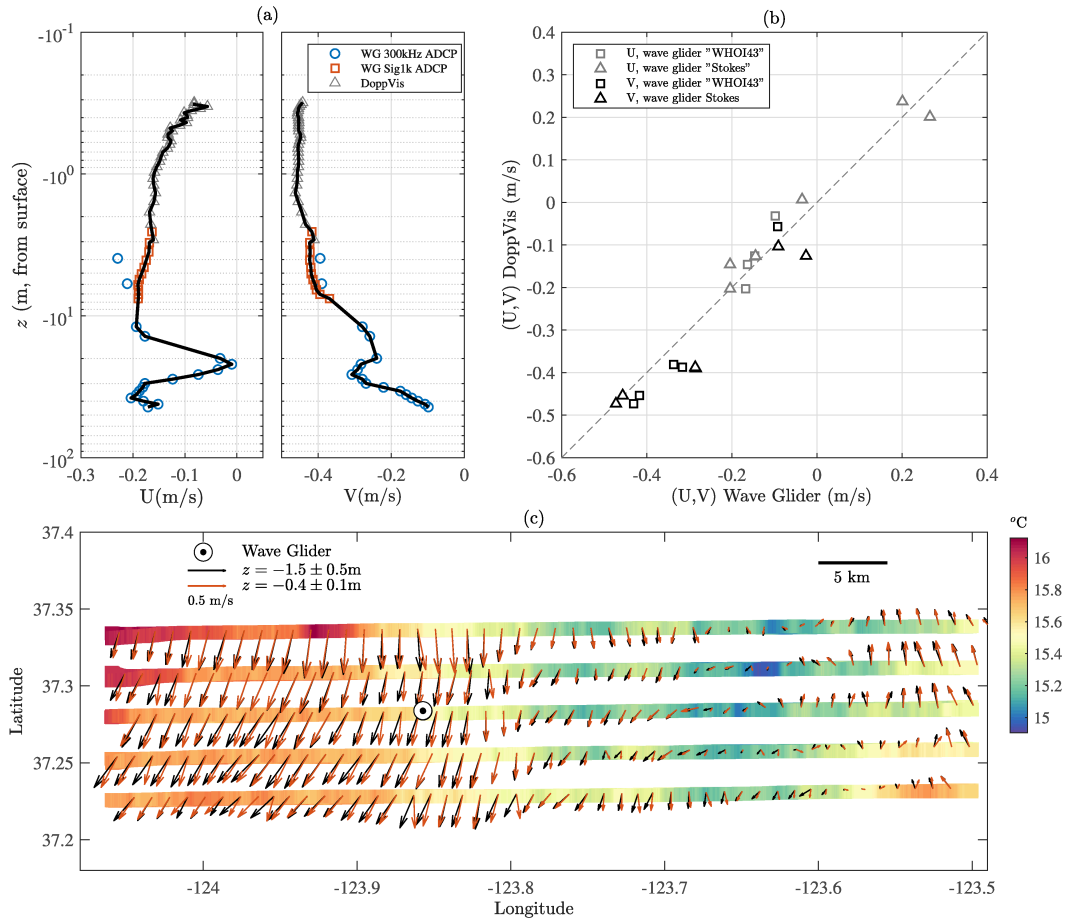

Figure 1. (a) Current profiles (U, V) collected from DoppVis (gray triangles) during an overflight of an instrumented Wave Glider during the S-MODE experiment on 4 November 2021 at 17:20 UTC. The Wave Glider is equipped with an upward-looking Nortek Signature 1000 Acoustic Doppler Current Profiler [ADCP] (orange squares) and a downward-looking ADCP (Teledyne RDI Workhorse 300 kHz; blue circles). The location of the Wave Glider with respect to the DoppVis observations is shown in (c). (b) Comparison between in-situ observations of currents collected at a 2–3 m water depth obtained from DoppVis and two Wave Gliders, named WHOI43 and STOKES, for the times and locations of overflights (within 500 m) during the entire S-MODE experiment. (c) Airborne observations of Sea Surface Temperature collected from Modular Aerial Sensing System on 4 November 2021 over the entire domain along with current estimates (1 km along-track resolution) from DoppVis at two depths, deep, $z = -1.5 \pm 0.5$ m (black arrows) and shallow, $z = -0.4 \pm 0.1$ m (red arrows).

Currents modulate the properties of surface gravity waves both through *wave refraction* (e.g., Ardhuin et al., 2017; Bôas et al., 2020; Pizzo & Salmon, 2021; Romero et al., 2017, 2020) and *local effects* (Lenain & Pizzo, 2021; Rascle et al., 2016, 2017). This may include changes in wave direction as well as wave steepness. Modulations to wave steepness can lead to enhanced fluxes between the air and sea (Deike et al., 2017; Freilich & Mahadevan, 2021; Gula et al., 2022; Li et al., 2016; Smith et al., 2016; Verma & Sarkar, 2021; Vrećica et al., 2022). However, the time and length scales of these wave-current interactions may vary considerably; Kenyon (1971) showed ray curvature due to refraction scaled as c_g/ζ for c_g the wave group velocity and ζ the vertical vorticity of the current while local effects operate on spatial scales that go like U/c which may be $O(1)$ for shorter waves. Observationally, this requires the collection high-resolution measurements of currents and spectral wave properties over large areas of space to better understand wave-current interaction from meso- to submesoscales.

Figure 2 shows a subset of these observations, focusing on an area of the domain with significant submesoscale variability in ocean current magnitude and direction. We find large modulation of surface currents, at scales of 1–8 km associated with submesoscale variations within the mesoscale eddy. Panel (b) shows a sharp SST front at 32.885°N with a change in temperature of approximately 0.5°C, associated with a velocity gradient $\partial U/\partial x \approx 10f$, where f is the Coriolis frequency.

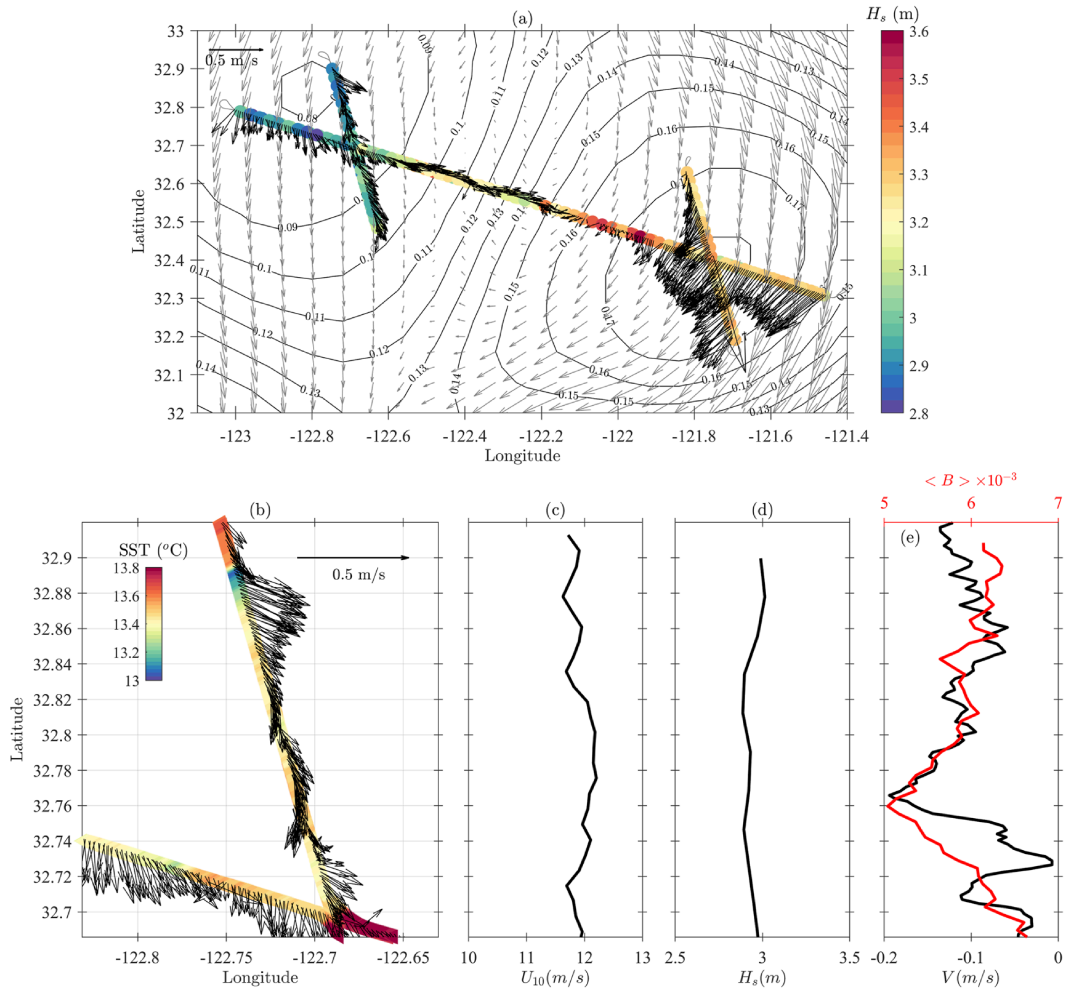

Figure 2. (a) Modular Aerial Sensing System significant wave height H_s and DoppVis surface current observations (250 m along-track resolution) collected during the Task Force Ocean experiment on 19 May 2021. The black contours represent the sea surface height (ssh, AVISO) at the time of the observations, while corresponding surface currents from HYCOM are shown as gray quivers. The larger scale trends of the surface currents are in general agreement with the HYCOM product, though the latter completely misses significant submesoscale features. We find significant modulation of the wave conditions across the domain, by up to 20%. (b) Subset of the data presented in (a) (northwestern part of the flight) with the track colorcoded for measured Sea Surface Temperature (SST). Note the strong modulation of surface currents over very short distances (1–8 km), coinciding in places with sharp SST fronts (e.g., at latitude around 32.885° in the northern part of the operation area). (c and d) show the wind speed U_{10} and significant wave height H_s collected along the North-northwest-South-southeast track shown in panel (b). (e) North component of the current V and mean spectral saturation $\langle B \rangle$, all plotted over the same range of latitude as in panel (b). Note the modulation of $\langle B \rangle$ associated with changes in V, the component of the current aligned with the waves, hinting at local wave-current interaction.

Figure 2c shows an approximately constant surface wind and significant wave height (Figure 2d) as a function of latitude on this transect. The classical arguments of Phillips (1985) then imply that the saturation spectrum, which characterizes the shorter waves in the spectrum which support most of the stress between the air and sea, should be constant. However, Figure 2e shows that the mean spectral saturation $\langle B \rangle$ (Romero et al., 2017) had significant variation. More formally, the saturation spectrum is defined as $B = \phi(k)k^3$, where ϕ is the omnidirectional wave spectrum (Phillips, 1984, 1985). The mean saturation is obtained by averaging B over the saturation range of the wave spectrum, with a lower bound k_n as defined in Lenain and Pizzo (2020; see also Pizzo et al., 2019). At that time, wind waves were approximately oriented in the same direction as the current V (Figure 2d).

Strikingly, we find that the mean saturation $\langle B \rangle$ generally follow the same evolution as V, which cannot be explained based on the classical arguments of Phillips (1985). A theoretical explanation of this phenomenon falls outside the scope of this manuscript and is being pursued elsewhere, but these novel observations motivate the

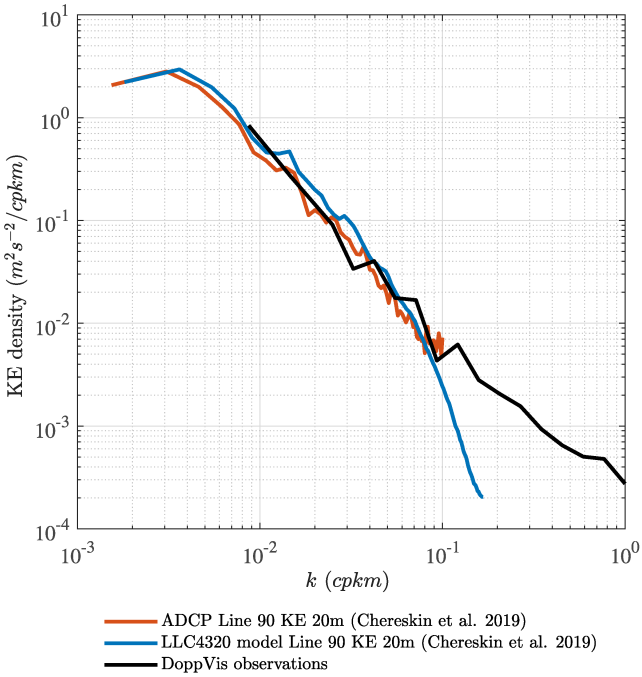

Figure 3. Comparison of kinetic energy spectra collected from the DoppVis Lagrangian surface currents on 19 May 2021 during one of the long East - West transects shown in Figure 2a compared with in-situ Acoustic Doppler Current Profiler observations (20 m depth) and LLC4320 hourly model products from Chereskin et al. (2019).

need to incorporate wave-current interactions into wave spectrum parameterizations, along the line of Lenain and Pizzo (2021) who investigated the use of Wentzel, Kramers and Brillouin method to predict the modulation of surface gravity waves by internal wave currents.

5. Transitions From Mesoscale to Submesoscale Motion

High-resolution measurements of surface currents enable the characterization of the transition between geostrophically balanced motion at larger scales and unbalanced (ageostrophic and wave) motion at smaller scales (Chereskin et al., 2019). In particular, determining the dynamics that predominate at the submesoscale has important implications for the vertical structure of the upper-ocean (Cronin et al., 2019) and the spatio-temporal distribution of energy dissipation (Ajayi et al., 2021; Buckingham et al., 2019; Dong et al., 2020; Schubert et al., 2020), and can lead to improvement of ocean-atmosphere coupled models (Li et al., 2016). While DoppVis observations are accurate enough to resolve submesoscale currents (horizontal resolution of less than 500 m), the airborne platform also travels quickly enough to collect nearly synoptic observations at the mesoscale (100 km). This is particularly valuable because it allows for examination of spatial variability across a range of scales and cross-scale interactions by not aliasing temporal variability.

Figure 3 shows kinetic energy (KE) spectra computed from the DoppVis surface current observations collected during one of the long East-West transects shown in Figure 2a compared with the average of 11 years of in-situ ADCP observations (20 m depth) and 1 year of LLC4320 hourly model products from Chereskin et al. (2019). The agreement at low wavenumbers (>10 km) is remarkable, as well as the fact that the KE spectrum from DoppVis maintains a nearly continuous slope for higher wavenumbers, down to 1 km scale. Feedbacks on ocean currents from wind and waves is likely important for determining dynamics at scales of less than 10 km where submesoscale processes predominate (Haney et al., 2015; Suzuki & Fox-Kemper, 2016; Yuan & Liang, 2021). Understanding these couplings needs to be advanced by direct observations that span scales from submesoscale to mesoscale. Characterization of the transition between geostrophically balanced motion and unbalanced dynamics is further explored in forthcoming work.

6. Velocity Gradient Statistics

Submesoscale dynamics are defined by the large velocity gradients at these scales, with $\mathcal{O}(1)$ Rossby number (McWilliams, 2016). Consistent with the small spatial scale of submesoscale dynamics, they also have fast temporal scales (Callies et al., 2020). Observations of not just velocity, but 2D velocity gradients of quickly evolving submesoscale features are therefore important for understanding submesoscale dynamics, but require synoptic observations over scales of tens of kilometers, which is not feasible with relatively slow-moving ship-based observations. Previous observations of submesoscale velocity gradients have used two ships (Shcherbina et al., 2013) or large drifter arrays (Berta et al., 2016; Essink et al., 2022). Aircraft-based observations offer a well-suited platform for studying submesoscale dynamics due to their fast speed relative to ships and high resolution measurements, generally higher than what is afforded by satellites.

In recent years, through numerical (Balwada et al., 2021) and observational (Shcherbina et al., 2013) studies, the surface vorticity–strain Joint Probability Density Function (JPDF) has been demonstrated as a useful tool to distinguish between different flow regimes, in particular in the context of submesoscale dynamics. In Figure 4, we show vorticity-strain and divergence-strain JPDFs computed from high-resolution 2D DoppVis surface current spatial observations collected during the S-MODE pilot experiment on October 2021 (60 km long section). During that portion of the flight, the aircraft flew at 3,000 ft AMSL, increasing the swath width of surface current observation up to 2 km, with a horizontal resolution (cross and along-track) of 128 m, in turn providing swath of the East and

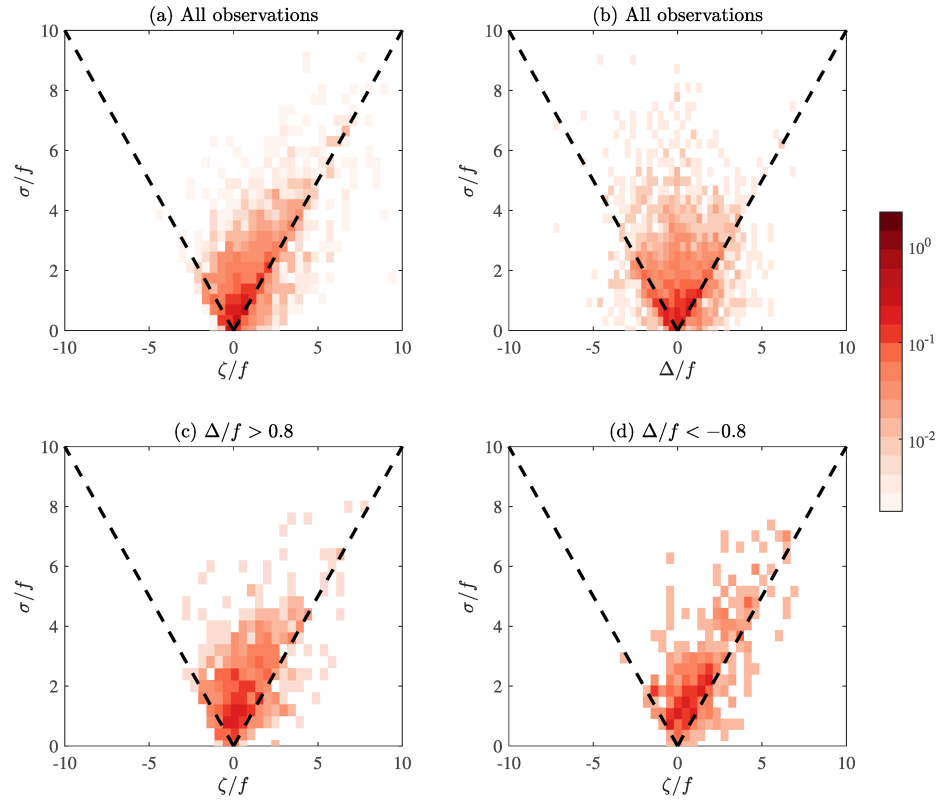

Figure 4. (a) Surface vorticity–strain and (b) divergence-strain JPDFs computed from 128 m resolution DoppVis products collected on 5 October 2021 during the S-MODE pilot program. (c and d) Surface vorticity–strain for $\Delta/f > 0.8$ and $\Delta/f < -0.8$ respectively. The dashed lines represents the lines $\sigma = \zeta$ (a, c and d) and $\sigma = \Delta$ (b), respectively.

North components of the surface velocity, $u(x, y)$ and $v(x, y)$ respectively, to compute velocity gradient statistics, that is, vorticity $\zeta = v_x - u_y$, strain rate (modulus of shear and normal strain) $\sigma = \sqrt{(v_x + u_y)^2 + (u_x - v_y)^2}$ and divergence $\Delta = u_x + v_y$. Overall, the distribution is skewed toward positive ζ/f values, with $\sigma/f > \zeta/f$ consistent with frontal structures, and classical submesoscale frontogenesis. This is particularly evident in panel (d), where the vorticity-strain JPDF for $\Delta/f < -0.8$ (i.e., convergence) is shown to be skewed to positive values. The same JPDF for positive values of Δ/f, larger than 0.8 (panel c) is not skewed toward negative ζ/f values, perhaps implying the contribution of other processes, for example, surface wave modulation properties and associated Stokes drift (recall that DoppVis observes Lagrangian current).

7. Discussions and Summary

We present unique coincident and collocated suborbital high-resolution observations of SST, surface currents and directional properties of surface waves collected from an airborne instrument (MASS), off the coast of Southern California, across submesoscales features.

- We have developed a novel airborne instrument, DoppVis, that enables coincident high-resolution observations of surface currents, vertical and horizontal shear alongside the other MASS instruments to capture quickly evolving features (both in time and space) such as submesoscale fronts, but also tidal estuarine flows, and more generally ocean phenomena that require frequent revisits and synoptic high resolution sampling (e.g., oil spills). The performances of this new instrument are carefully validated using in-situ observations, showing a bias of less than 1.5 cm/s and rms error of approximately 5 cm/s.
- Combining these observations with measurements of the properties of surface gravity waves allows for a careful examination of modulations to the surface wave field. In particular, we have shown that the saturation spectrum, which characterizes short surface waves that support most of the stress between the air and sea and facilitate air-sea interactions in general, is tightly coupled to the surface currents. This result cannot be

explained with conventional theoretical arguments and is a clear example of the power of the approach developed here for observing new ocean physics.

- Unprecedented broadband observations (from 1 to 100 km scale) of the KE spectrum of surface velocities are presented. This is a first step toward characterizing the transition between geostrophically balanced motion and unbalanced dynamics, further explored in forthcoming work.
- Surface vorticity–strain JPDFs computed from a 2D surface current maps collected from DoppVis is used to capture the different submesoscale flow regimes encountered at the time of our observations. We find consistency with our current understanding of frontal structures and classical submesoscale frontogenesis, and hints of the presence of other contributions, such as modulation of surface waves at the submesoscale (in turn, modulation of Stokes drift). Note, previous work has observationally investigated horizontal current gradients using slower moving platform (e.g., ships, Shcherbina et al., 2013), which is subject to significant spatio-temporal aliasing when attempting to characterize fast-evolving submesoscales currents. The results presented here show for the first time velocity gradient statistics of a *snapshot* of the ocean surface (aircraft takes 20 min to sample the 60 km swath analyzed here, vs. 6.5 hr for a research vessel surveying at a 5 kts speed).

Direct spatial and temporal observations of the lower atmosphere, sea surface and upper ocean are crucial for improved knowledge of air-sea interaction. However, the broad range of scales, or equivalently the strong spatial and temporal variability of theses interactions (see Figure 1), make this a formidable theoretical, numerical, and observational challenge. Traditional in-situ assets such as moorings and buoys are limited by their spatial coverage or their potential spatial biasing, in particular near an ocean front where buoys or drifters can cluster, while satellite imagery estimates important quantities like wind, significant wave height and currents through indirect methods and can also only sample at sparse time intervals. While limited observations and models have begun to reveal the coupling processes between ocean currents and wind (Chelton & Xie, 2010; Wenegrat & Arthur, 2018) and ocean currents and waves (Marechal & de Marez, 2022; Wang et al., 2020) at both the mesoscale and submesoscale, we need new observational technologies like MASS, DoppVis and DopplerScat (Rodríguez et al., 2018b) to unravel the underlying dynamics of these rapidly evolving processes.

Data Availability Statement

All presented data are available at UCSD Library Digital Collection, https://doi.org/10.6075/J0F76CRK.

Acknowledgments
We gratefully acknowledge useful comments from Ernesto Rodriguez and Roy Barkan. The authors are grateful to Twin Otter International for providing flight resources. This research was supported by grants from the Physical Oceanography programs at ONR (Grant N00014-19-1-2635), NASA (Grant 80NSSC19K1688) and NSF (OCE-2219752). SÅE acknowledges funding from the European Research Council (Grant 101045299) and the Research Council of Norway (Grant 325114).

References

Ajayi, A., Le Sommer, J., Chassignet, E. P., Molines, J.-M., Xu, X., Albert, A., & Dewar, W. (2021). Diagnosing cross-scale kinetic energy exchanges from two submesoscale permitting ocean models. *Journal of Advances in Modeling Earth Systems*, *13*(6), e2019MS001923. https://doi.org/10.1029/2019ms001923

Anderson, S. P., Zuckerman, S., Fan, S., & van Smirren, J. (2013). Airborne optical remote sensing of ocean currents. In *2013 oceans-San Diego* (pp. 1–7).

Ardhuin, F., Gille, S. T., Menemenlis, D., Rocha, C. B., Rascle, N., Chapron, B., et al. (2017). Small-scale open ocean currents have large effects on wind wave heights. *Journal of Geophysical Research: Oceans*, *122*(6), 4500–4517. https://doi.org/10.1002/2016jc012413

Balwada, D., Xiao, Q., Smith, S., Abernathey, R., & Gray, A. R. (2021). Vertical fluxes conditioned on vorticity and strain reveal submesoscale ventilation. *Journal of Physical Oceanography*, *51*(9), 2883–2901. https://doi.org/10.1175/jpo-d-21-0016.1

Balwada, D., Xie, J.-H., Marino, R., & Feraco, F. (2022). Direct observational evidence of an oceanic dual kinetic energy cascade and its seasonality. *Science Advances*, *8*(41), eabq2566. https://doi.org/10.1126/sciadv.abq2566

Barrick, D., & Weber, B. (1977). On the nonlinear theory for gravity waves on the ocean's surface. Part II: Interpretation and applications. *Journal of Physical Oceanography*, *7*(1), 11–21. https://doi.org/10.1175/1520-0485(1977)007<0011:otntfg>2.0.co;2

Belcher, S. E., Grant, A. L., Hanley, K. E., Fox-Kemper, B., Van Roekel, L., Sullivan, P. P., et al. (2012). A global perspective on Langmuir turbulence in the ocean surface boundary layer. *Geophysical Research Letters*, *39*(18), L18605. https://doi.org/10.1029/2012gl052932

Berta, M., Griffa, A., Özgökmen, T. M., & Poje, A. C. (2016). Submesoscale evolution of surface drifter triads in the Gulf of Mexico. *Geophysical Research Letters*, *43*(22), 11–751. https://doi.org/10.1002/2016gl070357

Bourassa, M. A., Meissner, T., Cerovecki, I., Chang, P. S., Dong, X., De Chiara, G., et al. (2019). Remotely sensed winds and wind stresses for marine forecasting and ocean modeling. *Frontiers in Marine Science*, *6*, 443. https://doi.org/10.3389/fmars.2019.00443

Broche, P., Demaistre, J., & Forget, P. (1983). Mesure par radar décamétrique cohérent des courants superficiels engendrés par le vent. *Oceanologica Acta*, *6*(1), 43–53.

Buckingham, C. E., Lucas, N. S., Belcher, S. E., Rippeth, T. P., Grant, A. L., Le Sommer, J., et al. (2019). The contribution of surface and submesoscale processes to turbulence in the open ocean surface boundary layer. *Journal of Advances in Modeling Earth Systems*, *11*(12), 4066–4094. https://doi.org/10.1029/2019ms001801

Bôas, A. B. V., Cornuelle, B. D., Mazloff, M. R., Gille, S. T., & Ardhuin, F. (2020). Wave–current interactions at meso-and submesoscales: Insights from idealized numerical simulations. *Journal of Physical Oceanography*, *50*(12), 3483–3500. https://doi.org/10.1175/jpo-d-20-0151.1

Callies, J., Barkan, R., & Garabato, A. N. (2020). Time scales of submesoscale flow inferred from a mooring array. *Journal of Physical Oceanography*, *50*(4), 1065–1086. https://doi.org/10.1175/jpo-d-19-0254.1

Campana, J., Terrill, E. J., & De Paolo, T. (2016). The development of an inversion technique to extract vertical current profiles from x-band radar observations. *Journal of Atmospheric and Oceanic Technology*, *33*(9), 2015–2028. https://doi.org/10.1175/jtech-d-15-0145.1

Cavaleri, L., Fox-Kemper, B., & Hemer, M. (2012). Wind waves in the coupled climate system. *Bulletin of the American Meteorological Society*, *93*(11), 1651–1661. https://doi.org/10.1175/bams-d-11-00170.1

Chelton, D. B., & Xie, S.-P. (2010). Coupled ocean-atmosphere interaction at oceanic mesoscales. *Oceanography*, *23*(4), 52–69. https://doi.org/10.5670/oceanog.2010.05

Chelton, D. B., Schlax, M. G., Freilich, M. H., & Milliff, R. F. (2004). Satellite measurements reveal persistent small-scale features in ocean winds. *Science*, *303*(5660), 978–983. https://doi.org/10.1126/science.1091901

Chereskin, T. K., Rocha, C. B., Gille, S. T., Menemenlis, D., & Passaro, M. (2019). Characterizing the transition from balanced to unbalanced motions in the southern California current. *Journal of Geophysical Research: Oceans*, *124*(3), 2088–2109. https://doi.org/10.1029/2018jc014583

Cronin, M. F., Gentemann, C. L., Edson, J., Ueki, I., Bourassa, M., Brown, S., et al. (2019). Air-sea fluxes with a focus on heat and momentum. *Frontiers in Marine Science*, *6*, 430. https://doi.org/10.3389/fmars.2019.00430

D'Asaro, E. A., Shcherbina, A. Y., Klymak, J. M., Molemaker, J., Novelli, G., Guigand, C. M., et al. (2018). Ocean convergence and the dispersion of flotsam. *Proceedings of the National Academy of Sciences*, *115*(6), 1162–1167. https://doi.org/10.1073/pnas.1718453115

Deike, L., Lenain, L., & Melville, W. K. (2017). Air entrainment by breaking waves. *Geophysical Research Letters*, *44*(12), 3779–3787. https://doi.org/10.1002/2017GL072883

Dewar, W. K., & Flierl, G. R. (1987). Some effects of the wind on rings. *Journal of Physical Oceanography*, *17*(10), 1653–1667. https://doi.org/10.1175/1520-0485(1987)017<1653:seotwo>2.0.co;2

Dong, J., Fox-Kemper, B., Zhang, H., & Dong, C. (2020). The seasonality of submesoscale energy production, content, and cascade. *Geophysical Research Letters*, *47*(6), e2020GL087388. https://doi.org/10.1029/2020gl087388

Dugan, J., & Piotrowski, C. (2003). Surface current measurements using airborne visible image time series. *Remote Sensing of Environment*, *84*(2), 309–319. https://doi.org/10.1016/s0034-4257(02)00116-5

Dugan, J., Piotrowski, C., & Williams, J. (2001). Water depth and surface current retrievals from airborne optical measurements of surface gravity wave dispersion. *Journal of Geophysical Research*, *106*(C8), 16903–16915. https://doi.org/10.1029/2000jc000369

Ellingsen, S. A., & Li, Y. (2017). Approximate dispersion relations for waves on arbitrary shear flows. *Journal of Geophysical Research: Oceans*, *122*(12), 9889–9905. https://doi.org/10.1002/2017jc012994

Essink, S., Hormann, V., Centurioni, L. R., & Mahadevan, A. (2022). On characterizing ocean kinematics from surface drifters. *Journal of Atmospheric and Oceanic Technology*, *39*(8), 1183–1198. https://doi.org/10.1175/jtech-d-21-0068.1

Fairall, C. W., Bradley, E. F., Rogers, D. P., Edson, J. B., & Young, G. S. (1996). Bulk parameterization of air-sea fluxes for tropical ocean-global atmosphere coupled-ocean atmosphere response experiment. *Journal of Geophysical Research*, *101*(C2), 3747–3764. https://doi.org/10.1029/95jc03205

Farrar, J. T., D'Asaro, E., Rodriguez, E., Shcherbina, A., Czech, E., Matthias, P., et al. (2020). S-mode: The sub-mesoscale ocean dynamics experiment. In *IGARSS 2020-2020 IEEE international geoscience and remote sensing symposium* (pp. 3533–3536).

Freilich, M., & Mahadevan, A. (2021). Coherent pathways for subduction from the surface mixed layer at ocean fronts. *Journal of Geophysical Research: Oceans*, *126*(5), e2020JC017042. https://doi.org/10.1029/2020jc017042

Grare, L., Statom, N. M., Pizzo, N., & Lenain, L. (2021). Instrumented wave gliders for air-sea interaction and upper ocean research. *Frontiers in Marine Science*, *8*, 664728. https://doi.org/10.3389/fmars.2021.664728

Gula, J., Taylor, J., Shcherbina, A., & Mahadevan, A. (2022). Submesoscale processes and mixing. In *Ocean mixing* (pp. 181–214). Elsevier.

Haney, S., Fox-Kemper, B., Julien, K., & Webb, A. (2015). Symmetric and geostrophic instabilities in the wave-forced ocean mixed layer. *Journal of Physical Oceanography*, *45*(12), 3033–3056. https://doi.org/10.1175/jpo-d-15-0044.1

Herbers, T. H. C., Jessen, P. F., Janssen, T. T., Colbert, D. B., & MacMahan, J. H. (2012). Observing ocean surface waves with GPS-tracked buoys. *Journal of Atmospheric and Oceanic Technology*, *29*(7), 944–959. https://doi.org/10.1175/jtech-d-11-00128.1

Huang, W., Carrasco, R., Shen, C., Gill, E. W., & Horstmann, J. (2016). Surface current measurements using x-band marine radar with vertical polarization. *IEEE Transactions on Geoscience and Remote Sensing*, *54*(5), 2988–2997. https://doi.org/10.1109/tgrs.2015.2509781

Kenyon, K. E. (1971). Wave refraction in ocean currents. *Deep-Sea Research and Oceanographic Abstracts*, *18*(10), 1023–1034. https://doi.org/10.1016/0011-7471(71)90006-4

Lenain, L., & Melville, W. K. (2014). Autonomous surface vehicle measurements of the ocean's response to tropical cyclone Freda. *Journal of Atmospheric and Oceanic Technology*, *31*(10), 2169–2190. https://doi.org/10.1175/jtech-d-14-00012.1

Lenain, L., & Melville, W. K. (2017). Measurements of the directional spectrum across the equilibrium saturation ranges of wind-generated surface waves. *Journal of Physical Oceanography*, *47*(8), 2123–2138. https://doi.org/10.1175/jpo-d-17-0017.1

Lenain, L., & Pizzo, N. (2020). The contribution of high frequency wind-generated surface waves to the Stokes drift. *Journal of Physical Oceanography*, *50*(12), 1–39. https://doi.org/10.1175/JPO-D-20-0116.1

Lenain, L., & Pizzo, N. (2021). Modulation of surface gravity waves by internal waves. *Journal of Physical Oceanography*, *51*(9), 2735–2748. https://doi.org/10.1175/jpo-d-20-0302.1

Lenain, L., Statom, N. M., & Melville, W. K. (2019). Airborne measurements of surface wind and slope statistics over the ocean. *Journal of Physical Oceanography*, *49*(11), 2799–2814. https://doi.org/10.1175/jpo-d-19-0098.1

Li, Q., Webb, A., Fox-Kemper, B., Craig, A., Danabasoglu, G., Large, W. G., & Vertenstein, M. (2016). Langmuir mixing effects on global climate: WAVEWATCH III in CESM. *Ocean Modelling*, *103*, 145–160. https://doi.org/10.1016/j.ocemod.2015.07.020

Longuet-Higgins, M. S., & Stewart, R. W. (1962). Radiation stress and mass transport in gravity waves, with application to 'surf beats'. *Journal of Fluid Mechanics*, *13*(4), 481–504.

Lund, B., Graber, H. C., Tamura, H., Collins, C., III, & Varlamov, S. (2015). A new technique for the retrieval of near-surface vertical current shear from marine x-band radar images. *Journal of Geophysical Research: Oceans*, *120*(12), 8466–8486. https://doi.org/10.1002/2015jc010961

Mahadevan, A. (2016). The impact of submesoscale physics on primary productivity of plankton. *Annual Review of Marine Science*, *8*(1), 161–184. https://doi.org/10.1146/annurev-marine-010814-015912

Marechal, G., & de Marez, C. (2022). Variability of surface gravity wave field over a realistic cyclonic eddy. *Ocean Science*, *18*(5), 1275–1292. https://doi.org/10.5194/os-18-1275-2022

McGillicuddy, D. J., Jr., Anderson, L. A., Bates, N. R., Bibby, T., Buesseler, K. O., Carlson, C. A., et al. (2007). Eddy/wind interactions stimulate extraordinary mid-ocean plankton blooms. *Science*, *316*(5827), 1021–1026. https://doi.org/10.1126/science.1136256

McWilliams, J. C. (2016). Submesoscale currents in the ocean. *Proceedings of the Royal Society A: Mathematical, Physical and Engineering Sciences*, *472*(2189), 20160117. https://doi.org/10.1098/rspa.2016.0117

Melville, W. K. (1996). The role of surface wave breaking in air-sea interaction. *Annual Review of Fluid Mechanics*, *28*(1), 279–321. https://doi.org/10.1146/annurev.fl.28.010196.001431

Melville, W. K., Lenain, L., Cayan, D. R., Kahru, M., Kleissl, J. P., Linden, P., & Statom, N. M. (2016). The modular aerial sensing system. *Journal of Atmospheric and Oceanic Technology*, *33*(6), 1169–1184. https://doi.org/10.1175/jtech-d-15-0067.1

Nouguier, F., Chapron, B., Collard, F., Mouche, A. A., Rascle, N., Ardhuin, F., & Wu, X. (2018). Sea surface kinematics from near-nadir radar measurements. *IEEE Transactions on Geoscience and Remote Sensing*, *56*(10), 6169–6179. https://doi.org/10.1109/tgrs.2018.2833200

O'Neill, L. W., Chelton, D. B., Esbensen, S. K., & Wentz, F. J. (2005). High-resolution satellite measurements of the atmospheric boundary layer response to SST variations along the Agulhas return current. *Journal of Climate*, *18*(14), 2706–2723. https://doi.org/10.1175/JCLI3415.1

Phillips, O. (1984). On the response of short ocean wave components at a fixed wavenumber to ocean current variations. *Journal of Physical Oceanography*, *14*(9), 1425–1433. https://doi.org/10.1175/1520-0485(1984)014<1425:otroso>2.0.co;2

Phillips, O. (1985). Spectral and statistical properties of the equilibrium range in wind-generated gravity waves. *Journal of Fluid Mechanics*, *156*(1), 505–531. https://doi.org/10.1017/s0022112085002221

Pizzo, N., Lenain, L., Rømcke, O., Ellingsen, S. Å., & Smeltzer, B. (2022). The role of Lagrangian drift in the geometry, kinematics and dynamics of surface waves. *Journal of Fluid Mechanics*, *954*, R4. https://doi.org/10.1017/jfm.2022.1036

Pizzo, N., Melville, W. K., & Deike, L. (2019). Lagrangian transport by nonbreaking and breaking deep-water waves at the ocean surface. *Journal of Physical Oceanography*, *49*(4), 983–992. https://doi.org/10.1175/jpo-d-18-0227.1

Pizzo, N., & Salmon, R. (2021). Particle description of the interaction between wave packets and point vortices. *Journal of Fluid Mechanics*, *925*, A32. https://doi.org/10.1017/jfm.2021.661

Rascle, N., Molemaker, J., Marié, L., Nouguier, F., Chapron, B., Lund, B., & Mouche, A. (2017). Intense deformation field at oceanic front inferred from directional sea surface roughness observations. *Geophysical Research Letters*, *44*(11), 5599–5608. https://doi.org/10.1002/2017gl073473

Rascle, N., Nouguier, F., Chapron, B., Mouche, A., & Ponte, A. (2016). Surface roughness changes by finescale current gradients: Properties at multiple azimuth view angles. *Journal of Physical Oceanography*, *46*(12), 3681–3694. https://doi.org/10.1175/jpo-d-15-0141.1

Rodríguez, E., Wineteer, A., Perkovic-Martin, D., Gál, T., Stiles, B. W., Niamsuwan, N., & Monje, R. R. (2018b). Estimating ocean vector winds and currents using a Ka-Band pencil-beam Doppler scatterometer. *Remote Sensing*, *10*(4), 576. https://doi.org/10.3390/rs10040576

Rodríguez, E., Wineteer, A., Perkovic-Martin, D., Gál, T., Stiles, B., Niamsuwan, N., & Monje, R. R. (2018a). Ocean surface currents and winds using Dopplerscatt. In *IGARSS 2018-2018 IEEE international geoscience and remote sensing symposium* (pp. 1474–1476).

Romero, L., Hypolite, D., & McWilliams, J. C. (2020). Submesoscale current effects on surface waves. *Ocean Modelling*, *153*, 101662. https://doi.org/10.1016/j.ocemod.2020.101662

Romero, L., Lenain, L., & Melville, W. K. (2017). Observations of surface wave–current interaction. *Journal of Physical Oceanography*, *47*(3), 615–632. https://doi.org/10.1175/jpo-d-16-0108.1

Schubert, R., Gula, J., Greatbatch, R. J., Baschek, B., & Biastoch, A. (2020). The submesoscale kinetic energy cascade: Mesoscale absorption of submesoscale mixed layer eddies and frontal downscale fluxes. *Journal of Physical Oceanography*, *50*(9), 2573–2589. https://doi.org/10.1175/jpo-d-19-0311.1

Shcherbina, A. Y., D'Asaro, E. A., Lee, C. M., Klymak, J. M., Molemaker, M. J., & McWilliams, J. C. (2013). Statistics of vertical vorticity, divergence, and strain in a developed submesoscale turbulence field. *Geophysical Research Letters*, *40*(17), 4706–4711. https://doi.org/10.1002/grl.50919

Smeltzer, B. K., & Ellingsen, S. Å. (2021). Current mapping from the wave spectrum. In W. Huang & E. W. Gill (Eds.), *Ocean remote sensing technologies: High frequency, marine and GNSS-based radar* (pp. 357–378). Institution of Engineering and Technology (IET). https://doi.org/10.1049/SBRA537E_ch15

Smeltzer, B. K., Æsøy, E., Ådnøy, A., & Ellingsen, S. Å. (2019). An improved method for determining near-surface currents from wave dispersion measurements. *Journal of Geophysical Research: Oceans*, *124*(12), 8832–8851. https://doi.org/10.1029/2019jc015202

Smith, K. M., Hamlington, P. E., & Fox-Kemper, B. (2016). Effects of submesoscale turbulence on ocean tracers. *Journal of Geophysical Research: Oceans*, *121*(1), 908–933. https://doi.org/10.1002/2015jc011089

Srinivasan, K., Barkan, R., & McWilliams, J. C. (2023). A forward energy flux at submesoscales driven by frontogenesis. *Journal of Physical Oceanography*, *53*(1), 287–305. https://doi.org/10.1175/jpo-d-22-0001.1

Stern, M. E. (1965). Interaction of a uniform wind stress with a geostrophic vortex. *Deep-Sea Research and Oceanographic Abstracts*, *12*(3), 355–367. https://doi.org/10.1016/0011-7471(65)90007-0

Stewart, R. H., & Joy, J. W. (1974). HF radio measurements of surface currents. *Deep-Sea Research and Oceanographic Abstracts*, *21*(12), 1039–1049. https://doi.org/10.1016/0011-7471(74)90066-7

Streßer, M., Carrasco, R., & Horstmann, J. (2017). Video-based estimation of surface currents using a low-cost quadcopter. *IEEE Geoscience and Remote Sensing Letters*, *14*(11), 2027–2031. https://doi.org/10.1109/lgrs.2017.2749120

Su, Z., Wang, J., Klein, P., Thompson, A. F., & Menemenlis, D. (2018). Ocean submesoscales as a key component of the global heat budget. *Nature Communications*, *9*(1), 1–8. https://doi.org/10.1038/s41467-018-02983-w

Sullivan, P. P., & McWilliams, J. C. (2010). Dynamics of winds and currents coupled to surface waves. *Annual Review of Fluid Mechanics*, *42*(1), 19–42. https://doi.org/10.1146/annurev-fluid-121108-145541

Suzuki, N., & Fox-Kemper, B. (2016). Understanding Stokes forces in the wave-averaged equations. *Journal of Geophysical Research: Oceans*, *121*(5), 3579–3596. https://doi.org/10.1002/2015jc011566

Thomas, M., Misra, S., Kambhamettu, C., & Kirby, J. T. (2005). A robust motion estimation algorithm for PIV. *Measurement Science and Technology*, *16*(3), 865–877. https://doi.org/10.1088/0957-0233/16/3/031

Toporkov, J. V., Perkovic, D., Farquharson, G., Sletten, M. A., & Frasier, S. J. (2005). Sea surface velocity vector retrieval using dual-beam interferometry: First demonstration. *IEEE Transactions on Geoscience and Remote Sensing*, *43*(11), 2494–2502. https://doi.org/10.1109/tgrs.2005.848603

Verma, V., & Sarkar, S. (2021). Lagrangian three-dimensional transport and dispersion by submesoscale currents at an upper-ocean front. *Ocean Modelling*, *165*, 101844. https://doi.org/10.1016/j.ocemod.2021.101844

Villas Bôas, A. B., Lenain, L., Cornuelle, B. D., Gille, S. T., & Mazloff, M. R. (2022). A broadband view of the sea surface height wavenumber spectrum. *Geophysical Research Letters*, *49*(4), e2021GL096699. https://doi.org/10.1029/2021gl096699

Vrećica, T., Pizzo, N., & Lenain, L. (2022). Observations of strongly modulated surface wave and wave breaking statistics at a submesoscale front. *Journal of Physical Oceanography*, *52*(2), 289–304. https://doi.org/10.1175/JPO-D-21-0125.1

Wang, J., Dong, C., & Yu, K. (2020). The influences of the Kuroshio on wave characteristics and wave energy distribution in the East China Sea. *Deep Sea Research Part I: Oceanographic Research Papers*, *158*, 103228. https://doi.org/10.1016/j.dsr.2020.103228

Wenegrat, J., & Arthur, R. (2018). Response of the atmospheric boundary layer to submesoscale sea surface temperature fronts. *Geophysical Research Letters*, *45*(24), 13–505. https://doi.org/10.1029/2018gl081034

Yuan, J., & Liang, J.-H. (2021). Wind-and wave-driven ocean surface boundary layer in a frontal zone: Roles of submesoscale Eddies and Ekman–Stokes transport. *Journal of Physical Oceanography*, *51*(8), 2655–2680. https://doi.org/10.1175/jpo-d-20-0270.1